



## Combination of pedCAT<sup>®</sup> for 3D Imaging in Standing Position With Pedography Shows No Statistical Correlation of Bone Position With Force/Pressure Distribution

Martinus Richter, MD, PhD<sup>1</sup>, Stefan Zech, MD<sup>2</sup>, Sarah Hahn, MD<sup>3</sup>,  
Issam Naef, MD<sup>3</sup>, David Mersch, MD<sup>3</sup>

<sup>1</sup> Professor and Surgeon, Department for Foot and Ankle Surgery, Rummelsberg and Nuremberg, Germany

<sup>2</sup> Head Attending Surgeon, Department for Foot and Ankle Surgery, Rummelsberg and Nuremberg, Germany

<sup>3</sup> Surgeon, Department for Foot and Ankle Surgery, Rummelsberg and Nuremberg, Germany

### ARTICLE INFO

*Level of Clinical Evidence:* Not applicable, diagnostic study without intervention

**Keywords:**  
3D imaging  
pedCAT<sup>®</sup>  
pedography  
bone position  
force distribution

### ABSTRACT

pedCAT<sup>®</sup> (CurveBeam, Warrington, PA) is a technology for 3-dimensional (3D) imaging with full weight-bearing that has been proved to exactly visualize the 3D bone position. For the present study, a customized pedography sensor (Pliance; Novel, Munich, Germany) was inserted into the pedCAT<sup>®</sup>. The aim of our study was to analyze the correlation of the bone position and force/pressure distribution. A prospective consecutive study of 50 patients was performed, starting July 28, 2014. All patients underwent a pedCAT<sup>®</sup> scan and simultaneous pedography with full weightbearing in the standing position. The following parameters were measured on the pedCAT<sup>®</sup> image for the right foot by 3 different investigators 3 times: lateral talo-first metatarsal angle, calcaneal pitch angle, and minimum height of the fifth metatarsal base, second to fifth metatarsal heads, and medial sesamoid. From the pedography data, the following parameters were defined using the standardized software algorithm: midfoot contact area, maximum force of midfoot, maximum force of midfoot lateral, maximum force of entire foot, and maximum pressure of first to fifth metatarsal. The values of the corresponding pedCAT<sup>®</sup> and pedographic parameters were correlated (Pearson). The intra- and inter-observer reliability of the pedCAT<sup>®</sup> measurements were sufficient (analysis of variance,  $p > .8$  for each, power  $> 0.8$ ). No sufficient correlation was found between the pedCAT<sup>®</sup> and pedographic parameters ( $r < 0.05$  or  $r > -0.38$ ). 3D bone position did not correlate with the force and pressure distribution under the foot sole during simultaneous pedCAT<sup>®</sup> scanning and pedography. Thus, the bone positions measured with pedCAT<sup>®</sup> do not allow conclusions about the force and pressure distribution. However, the static pedographic parameters also do not allow conclusions about the 3D bone position. Bone position and force/pressure distribution are important parameters for diagnostics, planning, and follow-up examinations in foot and ankle surgery.

© 2016 by the American College of Foot and Ankle Surgeons. All rights reserved.

Analyzing the position of the bones radiographically allows conclusions to be drawn regarding the biomechanics of the foot (1–8). However, static and dynamic pedography is more effective for analysis of the biomechanics of the foot (5,9–11).

pedCAT<sup>®</sup> (CurveBeam, Warrington, PA) is a new technology that allows 3-dimensional (3D) imaging with full weightbearing that should be not influenced by the projection used or the foot

orientation (Figs. 1 and 2) (4). In an earlier study, specific bone position (angle) measurements with pedCAT<sup>®</sup> were compared with the measurements from conventional radiographs with weight-bearing and computed tomography (CT) without weightbearing (radiographs, CT, pedCAT<sup>®</sup>) (4). The angles differed among the radiographs, CT scans, and pedCAT<sup>®</sup> scans, and only pedCAT<sup>®</sup> was able to detect the correct angles (4). pedCAT<sup>®</sup> includes weight-bearing, in contrast to CT. Also, the use of pedCAT<sup>®</sup> prevents inaccuracies of projection and foot orientation owing to the 3D data set, which is principally independent of the projection and foot orientation, in contrast to radiographs (4). Pedography is a measurement of the force distribution under the sole of the foot and can be performed using a static or dynamic method (12,13). Over the years, a variety of methods has been used to study foot pressure (14–16). Many of these techniques have already improved our understanding of the foot and its function, and have had an effect on clinical

**Financial Disclosure:** None reported.

**Conflict of Interest:** Martinus Richter is consultant of Curvebeam, Stryker, Ulrich, and Intercus; proprietor of R-Innovation; and joint proprietor of First Worldwide Orthopaedics. Stefan Zech, Sarah Hahn, Issam Naef, and David Mersch reported no conflict of interest.

Address correspondence to: Martinus Richter, MD, PhD, Department for Foot and Ankle Surgery Rummelsberg and Nuremberg, Location Hospital Rummelsberg, Rummelsberg 71, Schwarzenbruck 90592, Germany.

E-mail address: martinus.richter@sana.de (M. Richter).

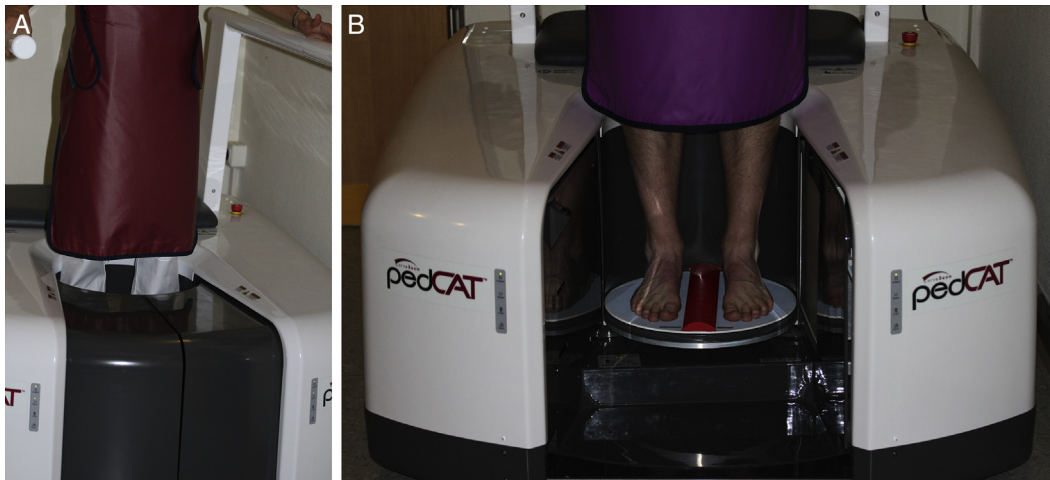


**Fig. 1.** pedCAT<sup>®</sup> with pedography sensor. An x-ray emitter and a flat panel sensor on the opposite side rotate horizontally around the feet. Resolution and contrast, which are the principal parameters for image quality, are comparable to those with modern conventional computed tomography. (A) A patient positioned in the pedCAT<sup>®</sup> during a scan. A sitting position is also possible for patients who are not allowed or are unable to stand. The gray part is the sliding door, which is opened before and after the scan to allow the patient entry and exit. The patient can walk into the device when the door is open. (B) The pedCAT<sup>®</sup> device with the sliding door open.

practice (5,9,14,17). The correlation between the 3D bone position and pedographic measurements (i.e., force and pressure [distribution]) has not been to date. For the present study, a customized pedography sensor (Pliance; Novel, Munich, Germany) was inserted into the pedCAT<sup>®</sup>. The aim of the present study was to analyze the correlation between the bone position and the force/pressure distribution.

**Patients and Methods**

A total of 50 patients were included in a prospective consecutive study starting July 28, 2014. A pedCAT<sup>®</sup> scan with simultaneous pedography of both feet

under full weightbearing in standing position was performed. There were 22 (44%) males and 28 (56%) females in the cohort, with a mean age of 48.4 ± 15.1 years. A customized pedography sensor (Pliance; Novel) was inserted into the pedCAT<sup>®</sup> and connected to a personal computer with the standard software installed (Expert; Novel). The potential pathologic features of the feet were registered but not further analyzed.

*Inclusion and Exclusion Criteria and Ethics*

The inclusion criteria were age ≥18 years, presentation at the local foot and ankle outpatient clinic, and indication for pedCAT<sup>®</sup>. The indication for pedCAT<sup>®</sup> was defined in accordance with the local standard (4). For example, no indication for 3D imaging with pedCAT<sup>®</sup> was given for isolated forefoot deformities. However, deformities in the

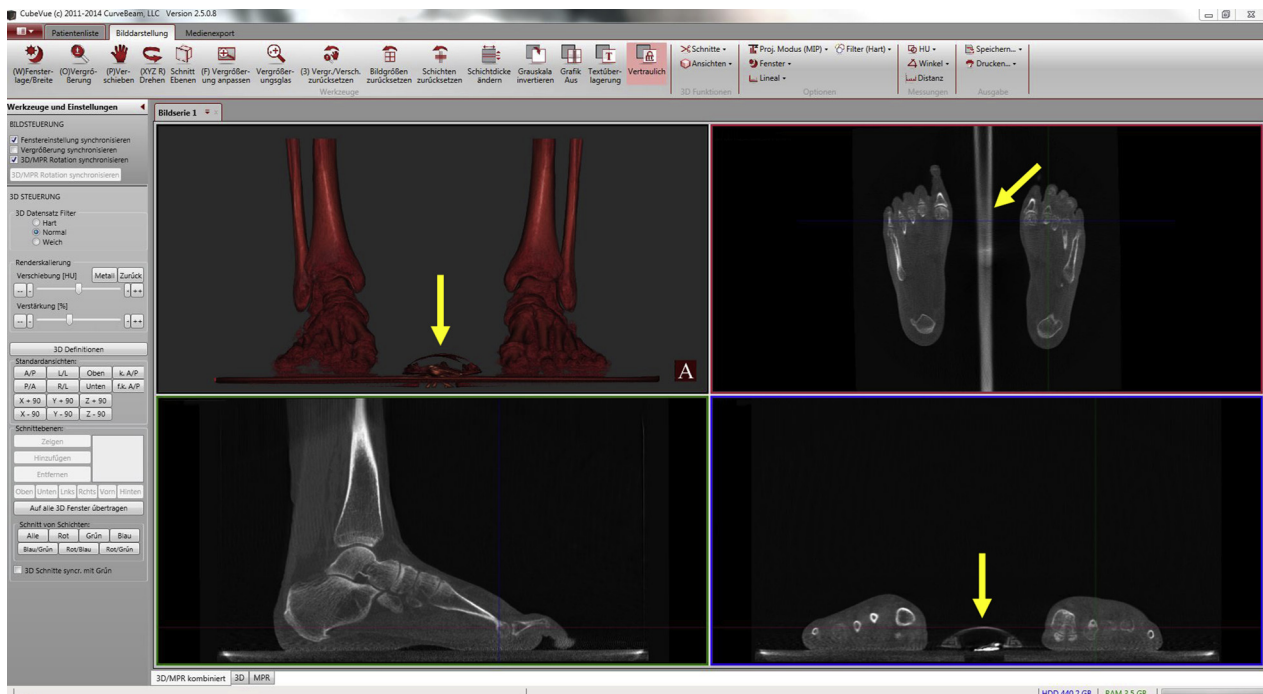


**Fig. 2.** pedCAT<sup>®</sup> software screen view with 3-dimensional reformation (top left), axial reformation (top right, red frame), parasagittal reformation (bottom left, green frame), and coronal reformation (bottom right, blue frame). The standard view is with a 1-mm slice thickness. The red lines (bottom left and bottom right) correspond to the axial reformation in the red frame (top right), the green lines (top right and bottom right) correspond to the parasagittal reformation in the green frame (bottom left), and the blue lines (bottom left and top right) correspond to the coronal reformation in the blue frame (bottom right). The arrows indicate the illustration of the pedography sensor hardware.

midfoot and/or hindfoot region were considered an indication for pedCAT®. The exclusion criteria were age <18 years, no indication for pedCAT® imaging, and participation in other studies. The local ethical committee granted approval of the study on the basis of the inclusion and exclusion criteria. All the subjects provided informed consent.

**Image Acquisition**

The patient walked into the device, and was positioned in a bipedal standing position (Fig. 1A). Technically, an x-ray emitter and a flat panel sensor on the opposite side rotate horizontally around the feet. The resolution and contrast, which are the principal parameters for image quality, are comparable to those of modern conventional CT (4). The scanning time was 68 seconds.

**Pedography**

The pedography sensor (Fig. 1B) gathered data for the first 30 seconds of the pedCAT® scan.

**Measurements of Bone Position (Angles and Distances)**

The bone positions (angles and distances) were digitally measured with standard pedCAT® software (Cubevue; CurveBeam, Warrington, PA). The following angles and distances were measured for the right foot by 3 different investigators 3 times: lateral

talo-first metatarsal angle (TMT), calcaneal pitch angle, and minimum height of fifth metatarsal base, second to fifth metatarsal heads, and medial sesamoid. The medial sesamoid was chosen instead the first metatarsal head, because it is regularly closer to the foot sole or ground. The medial sesamoid was chosen instead of the lateral sesamoid, because it is less likely to completely dislocate from underneath the first metatarsal head in forefoot deformities such as hallux valgus (18,19).

The lateral TMT angle was defined as the angle created between the axis of the first metatarsal and the talus (Fig. 3A) (4,20). The plane for the measurement was virtually rotated within the 3D data set to achieve an exact congruency to the bone axis of talus and first metatarsal (Fig. 3A).

The calcaneal pitch angle was defined as the angle created between a straight line and a line between the lowest part of the posterior calcaneal process and the lowest part of the anterior calcaneal process (Fig. 3B) (4). The plane for the measurement was virtually rotated within the 3D data set to achieve an exact congruency to a parasagittal plane.

The bone axes (talus, first metatarsal) were defined as a straight line between the centers of the bones proximally and distally. These bone centers were defined by linear measurements (Fig. 3A). The TMT angles were considered to be negative for angle corresponding to a dorsiflexion (20).

The minimum height of the fifth metatarsal base, second to fifth metatarsal heads, and medial sesamoid was defined as the minimum distance between the footplate and the fifth metatarsal base (Fig. 3C), medial sesamoid (Fig. 3D), and second to fifth metatarsal heads (Fig. 3E), respectively. The plane for the measurement was virtually shifted within the 3D data set to display the lowest part of the relevant bone.



**Fig. 3.** pedCAT® software screens showing examples of some of the angle and distance measurements. (A) Lateral talo-first metatarsal angle (arrow). The plane for the measurement was virtually rotated within the 3-dimensional data set to achieve an exact congruency with the bone axis of talus and first metatarsal to result in the image shown. (B) Calcaneal pitch angle. (C) Minimum height of fifth metatarsal base to footplate. (D) Height of medial sesamoid. (E) Height of second to fifth metatarsal heads. The lines that define the centers of the bones proximally or distally are exactly 50% of the measured entire bone thickness.



Measurement of Pedographic Parameters

Standard computerized mapping to separate the distribution into the following foot regions was performed using the standard software (Automask; Novel): hindfoot, midfoot, first metatarsal head/sesamoids area, second metatarsal head, third metatarsal head, fourth metatarsal head, fifth metatarsal head, first toe, second toe, and third to fifth toes (Fig. 4) (21). This mapping process does not include manual determination of the landmarks (21). The outlines of the foot and the different regions were determined by the software program using an algorithm, as previously reported (16). This software algorithm is based on the geometric characteristics of a maximum pressure picture using an individual sensing threshold (21). The following parameters were registered within the defined foot regions: midfoot contact area, maximum force of midfoot, maximum force of midfoot lateral, maximum force of entire foot, and maximum pressure of first to fifth metatarsal head area. The maximum force of midfoot parameter was defined as the maximum force in the entire midfoot region (Fig. 4). The maximum force of the midfoot lateral parameter was defined as the maximum force in the lateral sensor row of the midfoot region (Fig. 4).

Correlation Analysis of pedCAT® Parameters With Pedographic Parameters

The lateral TMT, calcaneal pitch angle, and minimum height of the fifth metatarsal base were each correlated with the midfoot contact area, maximum force of midfoot, maximum force of midfoot lateral, and maximum force of the entire foot. The minimum height of the second to fifth metatarsal heads and medial sesamoid were correlated with the maximum pressure of the corresponding first to fifth metatarsal head areas.

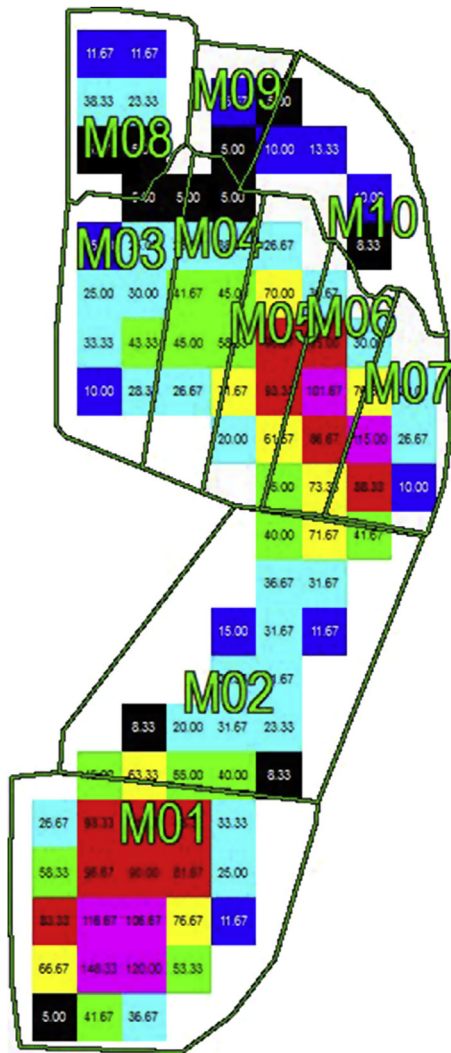


Fig. 4. Image from pedography after computerized mapping. The following regions were defined by the mapping process: M1, hindfoot; M2, midfoot; M3, first metatarsal head/sesamoids area; M4, second metatarsal head; M5, third metatarsal head; M6, fourth metatarsal head; M7, fifth metatarsal head; M8, first toe; M9, second toe; and M10, third to fifth toes.

Statistical Analysis

The statistical analysis was performed in cooperation with the Institute for Biometry and Statistics of the affiliated university using IBM® SPSS® Statistics, version 22.0.0.0 (IBM, Armonk, NY). The pedCAT® parameters were compared for intra- and interobserver (analysis of variance with post hoc Scheffe test). The correlation of the pedCAT® parameters with the pedographic parameters was performed using the Pearson test. A significant correlation was considered present at  $p \leq .05$ . Sufficient correlation was considered present at  $r > 0.8$  or  $r < -0.8$ .

Results

The descriptive statistics of all pedCAT® and pedographic parameters are listed in Table 1.

Measurements of Bone Position (Angles and Distances)—Intra- and Interobserver Reliability

Regarding intraobserver reliability, the angles and distances did not differ among measurements 1, 2, and 3 of all measured pedCAT® parameters for all 3 investigators (analysis of variance,  $p > .8$  for each, power  $> 0.8$ ). Regarding interobserver reliability, the angles and distances did not differ among the 3 investigators for measurements 1, 2, and 3 of all measured pedCAT® parameters (analysis of variance,  $p > .8$  for each, power  $> 0.8$ ).

Correlation of pedCAT® Parameters With Pedographic Parameters

Tables 2 and 3 list the correlation of the pedCAT® parameters with the pedographic parameters. The correlation between the angles and heights from the pedCAT® data with the force/pressure distribution from the pedographic data was not significant ( $p > .05$  for each), except for the TMT angle versus the midfoot contact area ( $p = .02$ ) and the maximum force of the entire foot ( $p = .01$ ) and the minimum height of the fifth metatarsal base versus the maximum force of the midfoot lateral ( $p = .05$ ). The correlation coefficient for these correlations was not sufficient (lateral TMT angle versus midfoot contact area,  $r = -0.32$ ; maximum force entire foot,  $r = 0.38$ ; and minimum height of fifth metatarsal base versus maximum force of midfoot lateral,  $r = -0.27$ ). In conclusion, no sufficient correlation was found.

Discussion

The present study is the first to analyze the direct correlation of the bone position and force/pressure distribution using simultaneous radiographic 3D imaging and pedography and full weightbearing. This correlation, as such, seems logical; however, it has not been shown from a scientific viewpoint.

Angle Measurement—Intra- and Interobserver Reliability

The intra- and interobserver reliability was sufficient for the measurements using pedCAT®. This probably resulted from using digital software-based measurements and the experience of all 3 investigators regarding these types of digital measurements. In the future, an automatic software based angular measurement between the bones in the 3D data set will be implemented. This will allow for investigator-independent analysis of these angles. The advantages of investigator-independent definitions of the parameters for pedography have been previously demonstrated (16).

Correlation of pedCAT® Parameters With Pedographic Parameters

The correlation between the angles and heights from the pedCAT® data with the force/pressure distribution from the pedographic data

**Table 1**  
Descriptive statistics of all measured pedCAT® and pedographic parameters (N = 50 patients)

	TL (°)	C (°)	H5P (mm)	H1 (mm)	H2 (mm)	H3 (mm)	H4 (mm)	H5 (mm)	MC (cm <sup>2</sup> )	MF (N)	MFLAT (N)	FMAX (N)	P1 (kPa)	P2 (kPa)	P3 (kPa)	P4 (kPa)	P5 (kPa)
Mean	-8.3	18.1	21.5	16.4	19.1	18.2	17.5	16.0	18.7	41.7	33.6	375.3	56.5	50.7	50.0	43.8	34.5
Min	-38.0	5.4	15.7	12.8	14.5	13.2	13.6	12.4	3.4	2.8	1.5	52.4	0.0	0.0	0.0	0.0	0.0
Max	14.3	33.5	47.4	28.2	25.9	26.6	25.8	25.4	44.0	203.5	112.8	563.2	355.0	120.0	103.3	100.0	256.7
SD	9.3	5.4	5.2	2.9	2.5	2.1	2.1	2.2	8.5	41.8	28.4	98.2	58.7	27.2	23.4	22.5	38.0

Abbreviations: C, calcaneal pitch angle; FMAX, maximum force of entire foot; H1, height of medial sesamoid; H2, H3, H4, and H5, height of second to fifth metatarsal head, respectively; H5P, minimum height of fifth metatarsal base; Max, maximum; MC, midfoot contact area; MF, maximum force of midfoot; MFLAT, maximum force of midfoot lateral; Min, minimum; SD, standard deviation; TL, lateral talo-first metatarsal angle.

was not significant, except for the lateral TMT angle versus midfoot contact area and maximum force of entire foot and minimum height of fifth metatarsal base versus maximum force of midfoot lateral. However, the correlation coefficient for these correlations was not sufficient, at -0.32, -0.38, and -0.27. In conclusion, no sufficient correlation was found. When analyzing all single cases in more detail, some typical associations between the bone position and pressure or force distribution were observed (Fig. 5). However, these case-limited parameters did not lead to statistically significant ( $p < .05$ ) or sufficient ( $r > 0.8$  or  $r < -0.8$ ) correlations. This finding was very surprising and disturbing. Everyone would expect, just as we did before performing the present study, that a high correlation must exist between the bone position and force/pressure distribution. We did extensively discuss the reasons for the missing statistical correlation within our study group. We could not find a convincing explanation. We wondered whether we had possibly chosen the wrong parameters. One could argue that parameters such as the lateral TMT angle or calcaneal pitch angle might not be appropriate. However, the height of the metatarsal heads, medial sesamoid, and proximal fifth metatarsal seem to be very comprehensive parameters for correlating the forces and pressures under these bony structures. We thought that different body weights might have influenced the results. Thus, we also used individual multiplication factors to standardize all pedographic parameters of the patients to a standard weight, or better, standard total force (data not shown). However, this also did not lead to any statistically sufficient correlations. No comparison of our results with the results from the published data was possible because no such measurements have been performed and reported.

**Study Limitations**

The shortcomings of the present study were not the typical ones, such as missing analyses of intra- and/or interobserver reliability or missing power analyses of the statistical test. The low case number might have been a shortcoming. However, we believe that a much higher case number would not have led to more significant correlations of pedCAT® parameters with the pedographic parameters. With 50 patients, we “reached” very low correlation coefficients of <0.4 (or

**Table 2**  
Correlation of pedCAT® parameters with pedographic parameters (N = 50 patients)

Variable	MC (cm <sup>2</sup> )	MF (N)	MFLAT (N)	FMAX (N)
TL (°)				
r Value	-0.32	-0.14	-0.14	-0.38
p Value	.02	.34	.33	.01
C (°)				
r Value	-0.11	-0.13	-0.11	0.00
p Value	.46	.37	.44	.98
H5P (mm)				
r Value	-0.24	-0.26	-0.27	0.06
p Value	.09	.07	.05	.68

Abbreviations: C, calcaneal pitch angle; FMAX, maximum force entire foot; H5P, minimum height fifth metatarsal base; MC, midfoot contact area, MF, maximum force midfoot; MFLAT, maximum force midfoot lateral; TL, lateral talo-first metatarsal angle.

>-0.4, respectively), which questions whether a greater case number would have led to a sufficient correlation of >0.8 or <-0.8. However, it is not clear that a higher case number would have led to a different level of significance and/or correlation. In some cases, high or higher case numbers “average” the data, diminishing the differences within the data and even decreasing a significance result, or, better, increasing the *p* value (22). We experienced this phenomenon in an earlier study of the with pedographic patterns of 461 subjects with different foot pathologic entities (22). When including all 461 subjects, no significant differences were found among the different pathology groups; however, significant differences were found when analyzing only specific subject groups (22).

The “exclusion” of forefoot deformities and the indication of pedCAT® for mid- and hindfoot deformities seems illogical and debatable. When we were planning the study, we found that the potential of the pedCAT® would be more relevant for the midfoot and hindfoot than for the forefoot, because we believe the forefoot, but not the mid- and hindfoot, can be adequately analyzed with plain radiography. At that point, the generation of radiographs from the pedCAT® data was not yet possible. Thus, we also obtained radiographs for all patients who had undergone a pedCAT® scan. Thus, for forefoot deformities, we did not wish to perform a pedCAT® scan and radiographs, because we did not consider the pedCAT® scan to be absolutely necessary. We also wish to ensure radiation protection. This indication strategy was also included in the application for ethical approval of the study, and the study design could not later be changed. To date, and after >1500 pedCAT® scans at our institution, the indications have been completely changed. We no longer perform conventional radiography but instead use only pedCAT® scans. We then generate the plain radiographs from the pedCAT® data. After performing all these scans, including for forefoot deformities, we

**Table 3**  
Correlation of pedCAT parameters with maximum pressure determined by pedography (N = 50 patients)

pedCAT Parameter	Pedographic Parameter				
	P1 (kPa)	P2 (kPa)	P3 (kPa)	P4 (kPa)	P5 (kPa)
H1 (mm)					
r Value	-0.02				
p Value	.90				
H2 (mm)					
r Value		-0.22			
p Value		.13			
H3 (mm)					
r Value			-0.11		
p Value			.45		
H4 (mm)					
r Value				-0.22	
p Value				.12	
H5 (mm)					
r Value					-0.14
p Value					.35

Abbreviations: H1, height of medial sesamoid; H2, H3, H4, H5, height of second to fifth metatarsal heads, respectively; P1, P2, P3, P4, P5, maximum pressure of first to fifth metatarsals, respectively.

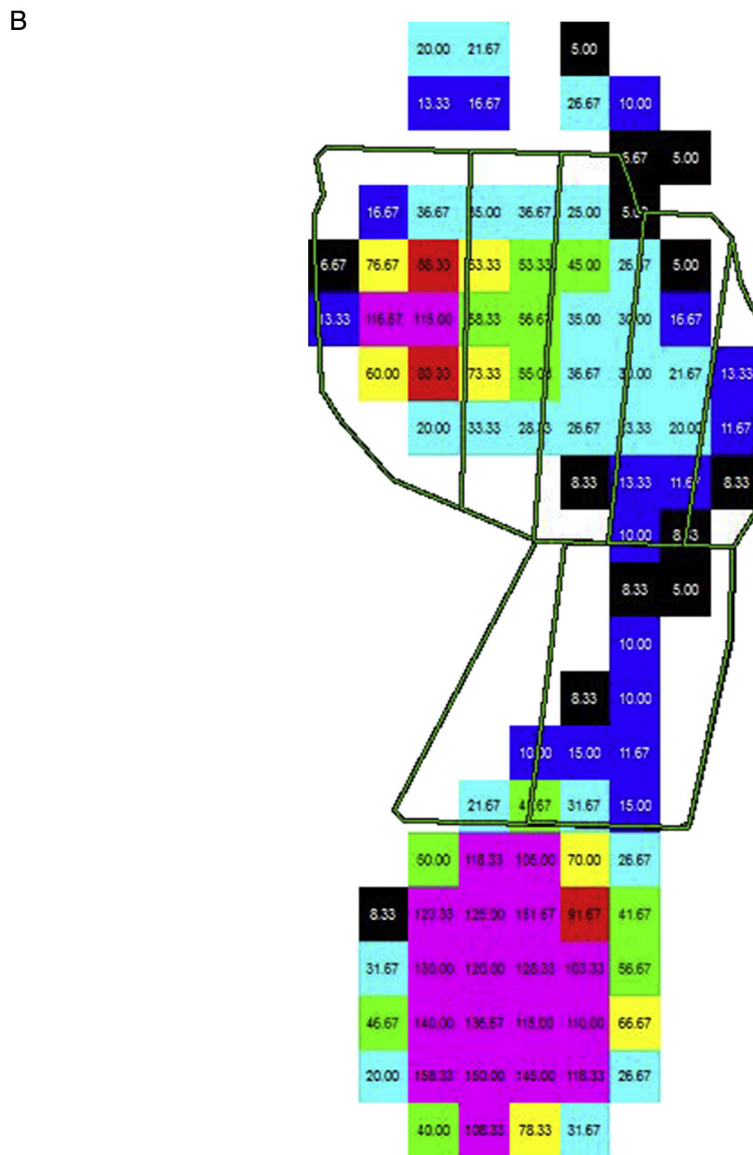
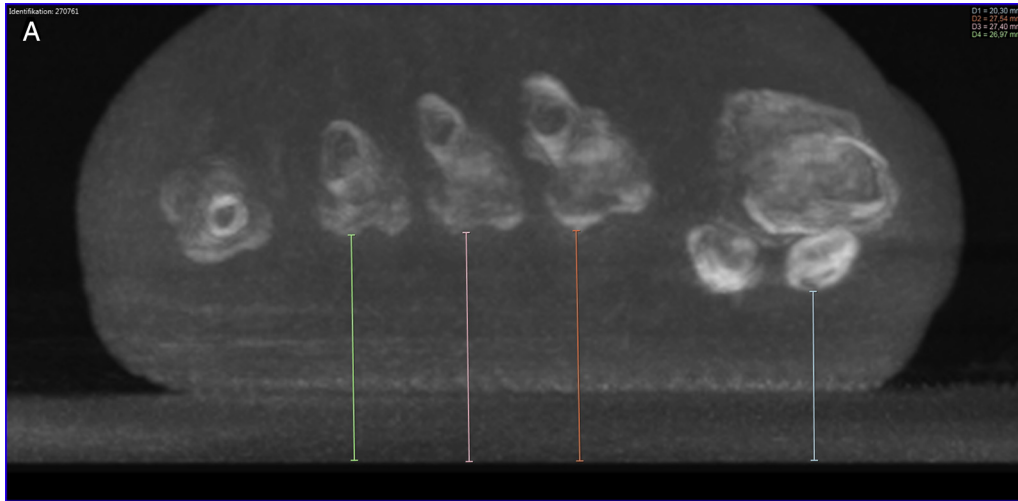


**Fig. 5.** Correlation of (A) pedCAT® (slice thickness increased for better visualization) and (B) pedography. The mean height of the medial sesamoid was 20.3 mm, and the mean height of the second to fifth metatarsals was greater (second, 27.6 mm; third, 27.4 mm; fourth, 27.0 mm; fifth, 26.4 mm, measurement not shown). The maximum pressure was 116.7 kPa for the first metatarsal and was lower for the second to fifth metatarsals (second, 73.3 kPa; third, 45.0 kPa; fourth, 30.0 kPa; fifth, 13.3 kPa). The lower first metatarsal and medial sesamoid resulted in greater pressure than did the higher second to fifth metatarsals.

strongly believe that 3D analysis of all foot deformities, including forefoot deformities, is useful.

We did not measure how difficult and time-consuming it was to measure the pedCAT<sup>®</sup> parameters. The reason was that the type and version of software and, above all, the experience of the investigator could have influenced the time required much more than would the method. Finally, the potential foot pathologic features of the subjects were registered but not analyzed. The pathologic angles (lateral TMT angle,  $-8.3^\circ$ ; calcaneal pitch angle,  $18.1^\circ$  on average) imply that relevant pathologic features were present, which was also determined by the inclusion criteria. However, we did not intend to investigate the different pathologic features but, instead, the correlation of the pedCAT<sup>®</sup> parameters with the pedographic parameters. Currently, pedography is a dynamic method used for the detection and analysis of the entire stance phase during gait, as well as in the standing position (i.e., static pedography). We measured the static quality of the foot, and we are aware that this is not directly related to the dynamic mechanics of the foot (4). We did not design the introduced method to mimic dynamic pedography (4). It has been previously shown and discussed that static pedography also allows conclusions about the biomechanics of the foot (4,5,12,13). However, the current basis for the standardized position in biomechanical radiography is to approximate the subjects' midstance angle and base of gait. To date, this is not possible with the pedCAT<sup>®</sup> unit. Further development of the pedCAT<sup>®</sup> technology to allow continuous 3D scanning during the entire stance phase of the gate is desirable. This development is already in progress and will require much faster detectors and a much larger device and the inclusion of some type of treadmill to allow for walking in the device. A dynamic scan would then allow one to analyze the bone position during the entire stance phase and to correlate the bone position with the "standard" dynamic pedographic data.

*Radiation Dose*

The radiation dose of the pedCAT<sup>®</sup> was not investigated in the present study. However, the radiation dose is a principal concern (4). Recently, the dose of foot and ankle radiographs, CT, and pedCAT<sup>®</sup> was measured and analyzed using a foot and ankle phantom (23). The dose for adults for 3 radiographs from 1 foot (dorsoplantar, lateral, and oblique views) was 0.7  $\mu$ Sv. The dose for a bilateral pedCAT<sup>®</sup> scan was 4.3  $\mu$ Sv, and the dose for conventional CT of 1 foot and ankle was 25  $\mu$ Sv (23). Thus, a bilateral pedCAT<sup>®</sup> scan has a dose comparable to that of 18 unilateral radiographs of the foot and 17% of a unilateral CT scan of the foot and ankle (23). That study also measured the dose of a unilateral pedCAT<sup>®</sup> scan, which was 1.4  $\mu$ Sv, comparable to 6 unilateral radiographs of the foot and 5.6% of a unilateral CT scan of the foot and ankle (23). For later clinical use, this radiation dose is relative, because virtual radiographs can be created from the pedCAT<sup>®</sup> data (4). We created the following virtual radiographs from the pedCAT<sup>®</sup> scan data: entire foot dorsoplantar and lateral views, ankle dorsoplantar, Mortise and lateral views, Saltzman views, metatarsal head skyline views, and Broden's views (all views were bilateral) (4).

In conclusion, the 3D bone position did not correlate with the force and pressure distribution under the foot sole during simultaneous pedCAT<sup>®</sup> scanning and pedography. Thus, the bone positions

measured using pedCAT<sup>®</sup> do not allow conclusions about the force and pressure distribution. However, the static pedographic parameters also do not allow conclusions about the 3D bone position. Additional investigations with greater case numbers and more parameters should be performed to further validate these surprising findings.

**References**

1. Easley ME, Trnka HJ, Schon LC, Myerson MS. Isolated subtalar arthrodesis. *J Bone Joint Surg Am* 82:613–624, 2000.
2. Marti RK, de Heus JA, Roolker W, Poolman RW, Besselaar PP. Subtalar arthrodesis with correction of deformity after fractures of the os calcis. *J Bone Joint Surg Br* 81:611–616, 1999.
3. Rammelt S, Grass R, Zawadski T, Biewener A, Zwipp H. Foot function after subtalar distraction bone-block arthrodesis: a prospective study. *J Bone Joint Surg Br* 86:659–668, 2004.
4. Richter M, Seidl B, Zech S, Hahn S. pedCAT for 3D-imaging in standing position allows for more accurate bone position (angle) measurement than radiographs or CT. *Foot Ankle Surg* 20:201–207, 2014.
5. Richter M, Zech S, Leonard J, Goldner Award 2009: intraoperative pedobarography leads to improved outcome scores: a level I study. *Foot Ankle Int* 30:1029–1036, 2009.
6. Trnka HJ, Easley ME, Lam PW, Anderson CD, Schon LC, Myerson MS. Subtalar distraction bone block arthrodesis. *J Bone Joint Surg Br* 83:849–854, 2001.
7. Zwipp H. *Biomechanik der Sprunggelenke*. Unfallchirurg 92:98–102, 1989.
8. Zwipp H. *Chirurgie des Fusses*, Springer, Heidelberg, New York, 1994.
9. Cavanagh PR, Henley JD. The computer era in gait analysis. *Clin Podiatr Med Surg* 10:471–484, 1993.
10. Cavanagh PR, Rodgers MM, Iiboshi A. Pressure distribution under symptom-free feet during barefoot standing. *Foot Ankle* 7:262–276, 1987.
11. Rosenbaum D, Becker HP, Sterk J, Gerngross H, Claes L. Functional evaluation of the 10-year outcome after modified Evans repair for chronic ankle instability. *Foot Ankle Int* 18:765–771, 1997.
12. Grieve DW, Rashdi T. Pressures under normal feet in standing and walking as measured by foil pedobarography. *Ann Rheum Dis* 43:816–818, 1984.
13. Inman VT, Ralston HJ, Todd F. *Human Walking*, Lippincott, Williams & Wilkins, Philadelphia, 1981.
14. Alexander IJ, Chao EY, Johnson KA. The assessment of dynamic foot-to-ground contact forces and plantar pressure distribution: a review of the evolution of current techniques and clinical applications. *Foot Ankle* 11:152–167, 1990.
15. Becker HP, Rosenbaum D, Zeithammer G, Gerngross H, Claes L. Gait pattern analysis after ankle ligament reconstruction (modified Evans procedure). *Foot Ankle Int* 15:477–482, 1994.
16. Cavanagh PR, Ulbrecht JS, Caputo GM. Elevated plantar pressure and ulceration in diabetic patients after panmetatarsal head resection: two case reports. *Foot Ankle Int* 20:521–526, 1999.
17. Rosenbaum D, Engelhardt M, Becker HP, Claes L, Gerngross H. Clinical and functional outcome after anatomic and nonanatomic ankle ligament reconstruction: Evans tenodesis versus periosteal flap. *Foot Ankle Int* 20:636–639, 1999.
18. Talbot KD, Saltzman CL. Assessing sesamoid subluxation: how good is the AP radiograph? *Foot Ankle Int* 19:547–554, 1998.
19. Yildirim Y, Cabukoglu C, Erol B, Esemeli T. Effect of metatarsophalangeal joint position on the reliability of the tangential sesamoid view in determining sesamoid position. *Foot Ankle Int* 26:247–250, 2005.
20. Richter M, Zech S. Lengthening osteotomy of the calcaneus and flexor digitorum longus tendon transfer in flexible flatfoot deformity improves talo-1st metatarsal-index, clinical outcome and pedographic parameter. *Foot Ankle Surg* 19:56–61, 2012.
21. Richter M, Frink M, Zech S, Vanin N, Geerling J, Droste P, Krettek C. Intraoperative pedography: a validated method for static intraoperative biomechanical assessment. *Foot Ankle Int* 27:833–842, 2006.
22. Richter M, Zech S, Kalpen A. Pedographic findings in 461 patients in a foot and ankle outpatient clinic—definition of standard pedographic patterns for typical pathologies. *J Foot Ankle Res* 1:024, 2008.
23. Ludlow BW, Ivanovic M. Weightbearing CBCT, MDCT, and 2D imaging dosimetry of the foot and ankle. *Int J Diagn Imaging* 1:1–9, 2014.